Original Research Article

Nigerian Journal of Biotechnology and Life Sciences
ISSN: 2814-0281
Vol. 3 No 2 (2026) p. 93 - 110
http://www.njbls.fud.edu.ng/

Response Surface Optimization of Reducing-Sugar Release and Bioethanol Production from Cassava Peels Using Oven-Assisted Acetic–Citric Acid Hydrolysis

Onwuakor, C. E.[1]* and Nwokafor, C. V.[2]

[1]Department of Microbiology, College of Natural Sciences, Michael Okpara University of Agriculture, Umudike, Nigeria.
[2]Department of Biotechnology, University of the West of Scotland, Scotland, United Kingdom.

*Corresponding Author: ce.onwuako@mouau.edu.ng

https://doi.org/10.67601/njbls.v3i2.31

Article into
Date received
05/07/2026
Date accepted
18/07/2026
Available online
04/09/2026

Keywords
Cassava peel; bioethanol; response surface methodology; *Saccharomyces cerevisiae*; oven-assisted hydrolysis

Abstract

Cassava processing generates large quantities of peel waste that is commonly discarded or burned, yet its high carbohydrate content makes it a candidate feedstock for fermentable-sugar and bioethanol production. This study examined the oven-assisted hydrolysis of cassava peels using a combined acetic–citric acid system, followed by fermentation of the hydrolysate with *Saccharomyces cerevisiae*. A three-factor, modified central composite design with 20 runs evaluated the effects of acetic–citric acid concentration (A), oven temperature (B), and hydrolysis time (C) on reducing-sugar concentration. Reducing-sugar concentrations ranged from 9.38 to 24.76 g/L. The fitted quadratic model was highly significant ($F = 47.50$, $p < 0.0001$) and explained 97.71% of the variation ($R^2 = 0.9771$; adjusted $R^2 = 0.9566$; predicted $R^2 = 0.8353$). Hydrolysis time exerted the strongest effect, followed by oven temperature and then acid concentration; the acid and temperature quadratic terms were significant, whereas none of the two-factor interactions was significant. The lack-of-fit was statistically significant ($p = 0.0001$), a consequence of the very small pure error of the highly repeatable center-point runs rather than gross model inadequacy, and the model predicted an independent validation condition to within 6.50%. Numerical optimization identified a high-yield validation condition of 2.72% acetic–citric acid, 151 °C and 78 min, with a model-predicted reducing-sugar concentration of 26.34 g/L; triplicate validation gave 24.63 ± 0.41 g/L. Fermentation of the optimized hydrolysate yielded a maximum ethanol concentration of 8.92 g/L at 96 h, with a slight decline thereafter. Oven-assisted mixed organic-acid hydrolysis is therefore a workable, laboratory-accessible route for converting cassava peel waste into fermentable sugars and ethanol.

Introduction

Interest in bioethanol from lignocellulosic and starch-rich agricultural residues has grown alongside the wider push for renewable transport fuels, since these feedstocks support decarbonization and fit naturally within circular-

bioeconomy goals (Holmatov et al., 2021; Broda et al., 2022; Woźniak et al., 2025). Worldwide, such residues are produced in enormous quantities, yet a large share is left unused, burned, or sent to landfill, representing an avoidable environmental burden and a missed opportunity for valorization (Koul et al., 2021; Awogbemi & Von Kallon, 2022). Residue-based bioethanol is promising, but its global contribution is constrained by feedstock availability, sustainability thresholds, and the land, water, and carbon footprints involved (Holmatov et al., 2021). The choice of feedstock and the efficiency of conversion therefore largely determine whether such a route can be deployed in practice.

Cassava peel is a strong candidate in this respect. Cassava processing generates large volumes of peel that retain carbohydrate fractions convertible into fermentable sugars (Mardina et al., 2021). Compositional studies describe it as a starch-rich, fibrous residue with notable cellulose and hemicellulose contents, making it a dual starch–lignocellulosic substrate (Permatasari et al., 2023; Thuppahige et al., 2023; Chukwudi et al., 2025). In cassava-based economies, Nigerian *garri* production being a clear example, recovering value from these waste streams offers both environmental and economic gains (Chukwudi et al., 2025).

Converting cassava peel into ethanol depends on pretreatment and hydrolysis that can break down its recalcitrant structure and release fermentable sugars (Escobar et al., 2020; Broda et al., 2022; Jayakumar et al., 2023). Pretreatment severity matters a great deal, because temperature, residence time, and acid concentration together set the balance between sugar release and sugar degradation (Escobar et al., 2020; Du Pasquier et al., 2024). Dilute-acid systems solubilize hemicellulose effectively and raise sugar recovery, but under harsh conditions they also drive degradation reactions that produce furans and organic acids (Ariffin et al., 2020; Świątek et al., 2020). The inhibitors formed this way, including furfural, hydroxymethylfurfural, vanillin, and other phenolics, hinder fermentative microorganisms and lower biocatalyst productivity, and remain one of the more stubborn limitations of the process (Jilani & Olson, 2023; Honarmandrad et al., 2024).

These drawbacks have steered attention toward milder pretreatments. Organic acids, in particular, have proven useful alternatives to inorganic acids, improving both sugar release and process economics in agro-residue systems (Gönen et al., 2021). Working with mixed vegetable waste, Dharmalingam et al. (2022) reported that acetic and citric acids improved lignin and hemicellulose removal and made cellulose more accessible to enzymes; acetic acid even outperformed hydrochloric acid in reducing-sugar yield once conditions were optimized. The broader trend in pretreatment research points the same way: lower toxic inputs, better saccharification, and biomass fractionation built into biorefinery designs that recover cellulose, hemicellulose, and lignin together (Broda et al., 2022; Cheng et al., 2023).

Several routes have already converted cassava peel into ethanol, including acid hydrolysis followed by *Saccharomyces cerevisiae* fermentation, simultaneous saccharification and fermentation, and alkaline pretreatment paired with *Zymomonas mobilis* (Mardina et al., 2021; Osemwengie et al., 2021; Permatasari et al., 2023). Hydrothermal treatment of garri-processing waste, for instance, sharply raised reducing-sugar concentrations, showing how strongly cassava residues respond to controlled thermal pretreatment (Chukwudi et al., 2025). To fine-tune such systems, researchers have relied heavily on response surface methodology, especially Box–Behnken designs, optimizing variables such as enzyme loading, time, pH, temperature, acid ratio, and solids content (Gönen et al., 2021; Osemwengie et al., 2021; Permatasari et al., 2023). Even so, scale-up remains constrained by long hydrolysis times, inhibitor management, and overall cost (Broda et al., 2022).

What has not been examined, however, is the combined use of acetic and citric acids under controlled oven heating for cassava-peel hydrolysis, and its capacity for mild, low-inhibitor sugar release remains unquantified. The present study addresses this gap. It models and optimizes how acid concentration, temperature, and

hydrolysis time jointly affect reducing-sugar production from cassava peel, and then evaluates fermentation of the optimized hydrolysate for bioethanol production.

Materials and methods

Study area

The study was carried out in the Biotechnology and Product Development Department, National Root Crops Research Institute (NRCRI), Umudike, Abia State, Nigeria. Cassava peels were obtained from NRCRI, Umudike, and all laboratory processing, hydrolysis, fermentation and analytical procedures were conducted under controlled laboratory conditions. An overview of the process is shown in Figure 1.

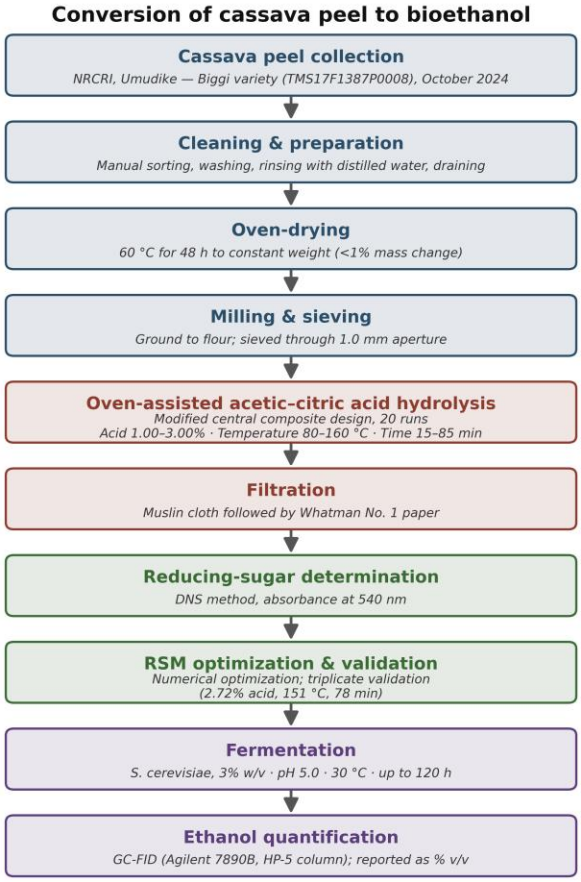

Figure 1: Process flow for the conversion of cassava peels to ethanol, from substrate preparation through oven-assisted acetic–citric acid hydrolysis and RSM optimization to fermentation and ethanol recovery.

Collection and preparation of cassava peels

Fresh cassava peels were collected from NRCRI, Umudike, Abia State, Nigeria, in October 2024. The cassava variety was Biggi (TMS17F1387P0008). The peels were sorted manually to remove sand, stones, woody materials and visibly decayed portions, washed thoroughly with clean water, rinsed with distilled water, and drained. The washed peels were oven-dried at 60 °C for 48 h until a constant weight was attained, defined as a mass change of less than 1% between two consecutive measurements taken after a further 2 h of drying. The dried peels were milled into flour using a locally fabricated dual-burr food grinder (Honda GX200 petrol prime mover, 6.5 hp at 3600 rpm; 150 mm chilled cast-iron grinding plates). The flour was sieved through a 1.0 mm aperture sieve, and the fraction passing the sieve was collected, stored in airtight containers and used for subsequent acetic–citric acid hydrolysis.

Preparation of the acetic–citric acid hydrolysis solution

Analytical-grade acetic acid (99.7% purity) and citric acid monohydrate (≥ 99.5% purity), both obtained from Ariaria Chemical Market, Aba, Abia State, Nigeria, were used. The combined use of acetic and citric acid as a mild organic-acid hydrolysis system was adapted from the organic-acid pretreatment and optimization approach described for mixed agricultural biomass by Dharmalingam et al. (2022), in which comparable organic acids were shown to hydrolyze biomass effectively while generating fewer inhibitory by-products than mineral acids. Separate 10% w/v stock solutions of acetic acid and of citric acid were prepared in distilled water. Equal volumes of the two stocks were combined (1:1 v/v) to form a mixed organic-acid stock, which was diluted with distilled water to give the working total-acid concentrations of 1.00%, 1.40%, 2.00%, 2.60% and 3.00% specified by the experimental design.

Oven-assisted acid hydrolysis

For each experimental run, 30 g of cassava peel flour was weighed into a 250 mL heat-resistant conical flask and treated with 100 mL of the appropriate acetic–citric acid solution (solid-to-liquid ratio 1:3.33 w/v), and the contents were mixed to form a uniform slurry. The flasks were covered with aluminum foil and placed in a thermostatically controlled hot-air oven (Zenith Lab, model DHG-9070A; temperature range 50–200 °C; chamber volume ≈ 70 L; timer 0–999 min). The use of oven heating to drive organic-acid hydrolysis, together with the temperature and time ranges investigated, followed the process-optimization framework applied to organic-acid biomass pretreatment by Gönen et al. (2021). Hydrolysis was conducted at the oven temperatures and exposure times set by the experimental design (acid concentration 1.00–3.00%; oven temperature 80–160 °C; hydrolysis time 15–85 min). After heating, each hydrolysate was cooled to room temperature and filtered through clean muslin cloth followed by Whatman No. 1 filter paper. The filtrate from each run was retained for reducing-sugar determination.

Determination of reducing sugar

Reducing-sugar concentration was determined by the 3,5-dinitrosalicylic acid (DNS) method, adapted for biomass hydrolysates following the reagent-to-sample ratio and heating protocol recommended by Wood et al. (2012) for the rapid and precise quantification of reducing sugars in biomass hydrolysates. The DNS reagent was prepared by dissolving 3,5-dinitrosalicylic acid (10 g), sodium hydroxide (10 g), sodium potassium tartrate (200 g), phenol (2 g) and sodium sulfite (0.5 g) in distilled water and making up to 1 L. For the assay, 1.0 mL of hydrolysate was mixed with 1.0 mL of DNS reagent, heated in a boiling water bath at 100 °C for 5 min, cooled to room temperature and diluted to 10 mL with distilled water. Absorbance was read at 540 nm using a single-beam UV-visible spectrophotometer (DLAB Scientific, model SP-UV1000; wavelength range 200–1000 nm; spectral bandwidth 4 nm). Reducing-sugar concentration was calculated from a glucose standard curve prepared over 0.20–2.00 g/L, with the calibration equation $A_{540} = 0.462C + 0.007$ and $R^2 = 0.9986$, where C is glucose concentration in g/L, and expressed as g/L.

Preparation of the yeast inoculum

Commercial baker's yeast (*Saccharomyces cerevisiae*; Royal Golden Crown Active baker's yeast), purchased from a bakery-supply outlet in Umuahia, Abia State, Nigeria, was used for fermentation. The yeast was activated by suspending 3.0 g of dry baker's yeast and 1.0 g of glucose in 50 mL of sterile distilled water at 35 °C for 20 min, following the yeast-activation procedure applied for cassava-peel bioethanol production by Osemwengie et al. (2021). The activated suspension was applied at 3% w/v dry-yeast equivalent and used immediately.

Fermentation of the cassava peel hydrolysate

A 100 mL portion of the hydrolysate obtained under the optimized hydrolysis conditions was transferred to a 250 mL conical flask and adjusted to pH 5.0 using sterile 1 M NaOH or 1 M HCl as required. The medium was inoculated with activated *Saccharomyces cerevisiae* at 3% w/v under

aseptic conditions. The batch fermentation conditions, including inoculum level, incubation temperature and sampling schedule, were adapted from protocols established for the fermentation of pretreated cassava-peel hydrolysates (Papathoti et al., 2021; Permatasari et al., 2023). Fermentation was carried out in flasks fitted with cotton plugs at 30 °C, with samples withdrawn at 24 h intervals up to 120 h. At each sampling point, the broth was centrifuged at 5000 rpm for 10 min and the clear supernatant collected for ethanol determination.

Determination of ethanol content

Ethanol concentration in the supernatant was determined by gas chromatography with flame-ionization detection (GC-FID) using an Agilent 7890B system fitted with an HP-5 capillary column (30 m × 0.32 mm i.d. × 0.25 μm film thickness). High-purity helium (99.999%) served as the carrier gas at a constant flow of 1.2 mL/min. Samples were introduced in split mode (split ratio 1:50) with the injector held at 250 °C and the flame-ionization detector at 280 °C. The column oven was programmed from an initial 60 °C (held for 1 min), ramped at 10 °C/min to 240 °C and held for 5 min. Ethanol was quantified against a calibration curve prepared from ethanol standards of known concentration, and results were expressed as grams of ethanol per liter (g/L).

Experimental design and RSM modeling

A modified, non-rotatable central composite design (CCD) was applied within response surface methodology to study the oven-assisted hydrolysis stage; the design is non-rotatable because the axial distances differed across the three factors ($\alpha \approx 1.67$ for acid concentration, 1.33 for oven temperature and 1.40 for hydrolysis time). This modified CCD/RSM framework for optimizing organic-acid-mediated biomass hydrolysis follows the design approach used in comparable cassava-peel and agro-waste bioethanol optimization studies (Osemwengie et al., 2021; Gönen et al., 2021). Twenty experimental runs were conducted, comprising eight factorial points, six axial points and six center-point replications. The three independent variables and their levels are summarized in Table 1; the response variable was reducing-sugar concentration (g/L). Factors were coded as A = (acid concentration − 2.00)/0.60, B = (oven temperature − 120)/30 and C = (hydrolysis time − 50)/25.

The relationship between the response and the independent variables was described by a second-order (quadratic) polynomial of the general form:

$$Y = \beta_0 + \beta_1 A + \beta_2 B + \beta_3 C + \beta_{11} A^2 + \beta_{22} B^2 + \beta_{33} C^2 + \beta_{12} AB + \beta_{13} AC + \beta_{23} BC \quad (1)$$

Where Y is the predicted reducing-sugar concentration; A, B and C are acetic–citric acid concentration, oven temperature and hydrolysis time, respectively; β_0 is the intercept; and the remaining β terms are the linear, quadratic and interaction coefficients.

Model adequacy was assessed by analysis of variance (ANOVA), the coefficient of determination (R^2), the adjusted R^2, the predicted R^2, the lack-of-fit test, and comparison of experimental and predicted responses.

Statistical analysis

Response surface modeling, ANOVA and numerical optimization were performed using Design-Expert software version 13. Model terms were considered statistically significant at $p < 0.05$. Center-point runs provided an estimate of pure error, and model adequacy was assessed by the lack-of-fit test and by R^2, adjusted R^2 and predicted R^2. The optimum condition obtained from the model was verified experimentally in triplicate.

Results and Discussion

Experimental design and reducing-sugar yield

Across the twenty runs of the central composite design, reducing-sugar concentration ranged from 9.38 to 24.76 g/L (Table 1). The lowest value (9.38 g/L) was recorded at the lowest factorial combination of acid concentration, oven temperature and hydrolysis time (1.40%, 90 °C, 25 min; Run 1), while the highest value (24.76 g/L)

occurred at the highest factorial combination (2.60%, 150 °C, 75 min; Run 8). The six center-point runs (Runs 15–20) gave closely grouped responses of 18.37–18.71 g/L, indicating good repeatability.

Table 1: Modified central composite design matrix for oven-assisted acetic–citric acid hydrolysis of cassava peels, with experimental and model-predicted reducing-sugar (RS) concentrations.

Run	Acid (%)	Oven temp. (°C)	Time (min)	Exp. RS (g/L)	Pred. RS (g/L)
1	1.4	90	25	9.38	8.26
2	2.6	90	25	12.44	11.94
3	1.4	150	25	13.27	13.15
4	2.6	150	25	17.86	17.43
5	1.4	90	75	14.18	14.45
6	2.6	90	75	18.92	18.89
7	1.4	150	75	20.34	20.68
8	2.6	150	75	24.76	25.72
9	1.0	120	50	12.83	13.13
10	3.0	120	50	20.47	20.39
11	2.0	80	50	11.96	12.94
12	2.0	160	50	21.38	20.75
13	2.0	120	15	10.74	12.22
14	2.0	120	85	23.52	22.36
15	2.0	120	50	18.64	18.52
16	2.0	120	50	18.37	18.52
17	2.0	120	50	18.71	18.52
18	2.0	120	50	18.55	18.52
19	2.0	120	50	18.42	18.52
20	2.0	120	50	18.69	18.52

Runs 1–8, factorial points; Runs 9–14, axial points; Runs 15–20, center points.

Regression model for reducing-sugar production

The fitted quadratic model indicated that all three factors influenced reducing-sugar release, with hydrolysis time and oven temperature contributing more strongly than acid concentration. The coded regression equation, obtained by least-squares fitting of the second-order model to the experimental reducing-sugar data, is given in equation 2. Agreement between predicted and experimental values is shown in Figure 2, and model diagnostics in Figure 3.

Analysis of variance

The analysis of variance (Table 2) showed that the quadratic model was highly significant ($F = 47.50$; $p < 0.0001$) and explained 97.71% of the variation in reducing-sugar concentration. Among the linear terms, hydrolysis time (C) had the largest partial sum of squares (156.14; $p < 0.0001$), followed by oven temperature (B; 99.27; $p < 0.0001$) and acid concentration (A; 64.39; $p < 0.0001$), confirming the factor ranking time > temperature > acid. None of the two-factor interactions was significant (AB, $p = 0.6410$; AC, $p = 0.5619$; BC, $p = 0.3103$). Of the quadratic terms, the acid and temperature terms were significant (A^2, $p = 0.0230$; B^2, $p = 0.0159$), whereas the hydrolysis-time quadratic term was not significant at the 5% level (C^2, $p = 0.0678$). The lack-of-fit was statistically significant ($F = 76.98$; $p = 0.0001$); as considered in the discussion, this reflects the very small pure error of the highly repeatable center-point runs rather than substantial model inadequacy, and the model retained strong predictive statistics and validated closely against an independent experiment.

$$Y = 18.52 + 2.18A + 2.93B + 3.62C + 0.15AB + 0.19AC + 0.34BC - 0.63A^2 - 0.94B^2 - 0.63C^2 \quad (2)$$

where A, B and C are the coded acetic–citric acid concentration, oven temperature and hydrolysis time respectively,

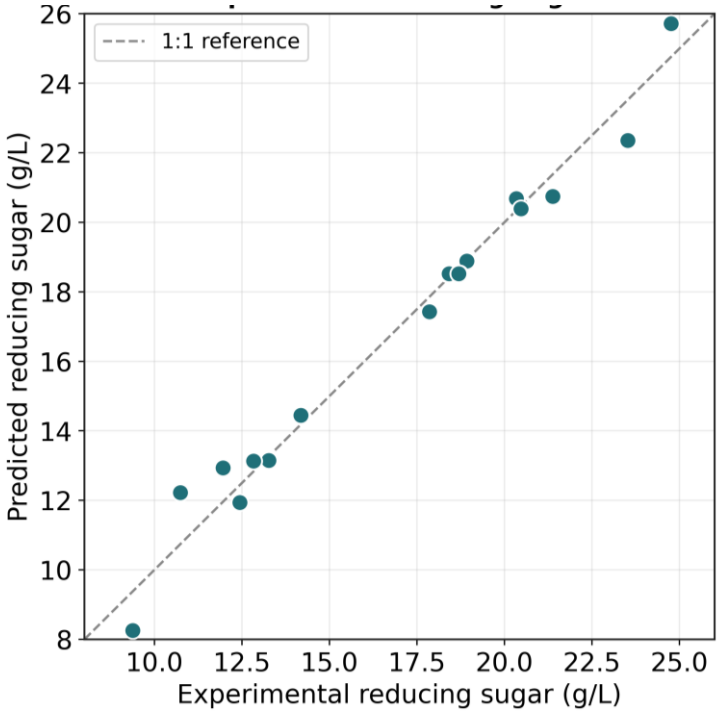

Figure 2: Predicted versus experimental reducing-sugar concentration for the twenty-run central composite design; the dashed line is the 1:1 reference.

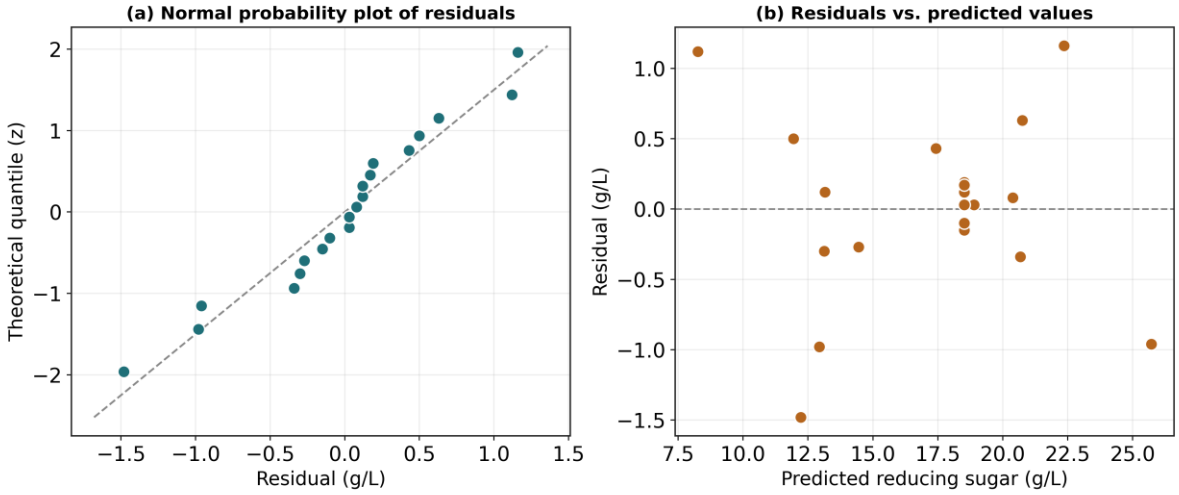

Figure 3: Model diagnostics: (a) normal probability plot of residuals; (b) residuals versus predicted reducing-sugar concentration.

Table 2: Analysis of variance for the fitted quadratic model for reducing-sugar production.

Source	df	Sum of squares	Mean square	F-value	p-value
Model	9	338.5	37.61	47.5	< 0.0001
A: acid concentration	1	64.39	64.39	81.32	< 0.0001
B: oven temperature	1	99.27	99.27	125.38	< 0.0001
C: hydrolysis time	1	156.14	156.14	197.21	< 0.0001
AB	1	0.18	0.18	0.23	0.641
AC	1	0.29	0.29	0.36	0.5619
BC	1	0.9	0.9	1.14	0.3103
A^2	1	5.7	5.7	7.2	0.023
B^2	1	6.65	6.65	8.4	0.0159
C^2	1	3.32	3.32	4.19	0.0678
Residual	10	7.92	0.792		
Lack of fit	5	7.82	1.563	76.98	0.0001
Pure error	5	0.102	0.0203		
Corrected total	19	346.41			

Individual model-term sums of squares are partial (Type III) sums of squares and are not expected to sum to the model sum of squares for this non-orthogonal design.

Table 3: Model-fit statistics for the quadratic model.

Parameter	**Value**
R^2	0.9771
Adjusted R^2	0.9566
Predicted R^2	0.8353
Standard deviation (g/L)	0.8898
Mean response (g/L)	17.1715
Coefficient of variation (%)	5.18
PRESS	57.05
Adequate precision	27.75

The model explained 97.71% of the variation in reducing-sugar concentration ($R^2 = 0.9771$), with an adjusted R^2 of 0.9566 and a predicted R^2 of 0.8353. The coefficient of variation was 5.18%, and the adequate precision of 27.75 greatly exceeded the conventional threshold of 4, indicating an adequate signal-to-noise ratio for navigating the design space.

Effects of the individual factors

At the central oven temperature and hydrolysis time, reducing-sugar concentration increased from 12.83 g/L at 1.00% acid to 20.47 g/L at 3.00% acid (Runs 9 and 10). At the central acid concentration and time, it increased from 11.96 g/L at 80 °C to 21.38 g/L at 160 °C (Runs 11 and 12). At the central acid concentration and temperature, it increased from 10.74 g/L at 15 min to 23.52 g/L at 85 min (Runs 13 and 14); hydrolysis time showed the largest single effect, consistent with its highest partial sum of squares in Table 2. The relative influence of the three factors is illustrated in the perturbation plot (Figure 4).

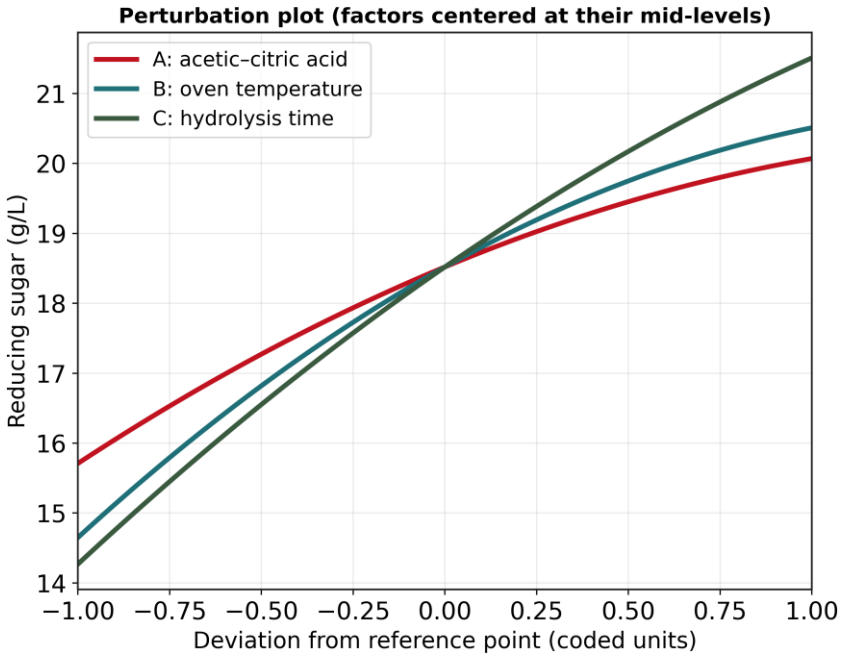

Figure 4: Perturbation plot showing the effect of each coded factor (A, acid concentration; B, oven temperature; C, hydrolysis time) on reducing-sugar concentration, with the other factors held at their center points.

Response surface trends

Figure 5 shows the combined effect of oven temperature and hydrolysis time on reducing-sugar production at a fixed acetic–citric acid concentration of 2.00%. Figure 6 shows the combined effect of acetic–citric acid concentration and oven temperature at a fixed hydrolysis time of 50 min, and Figure 7 shows the combined effect of acetic–citric acid concentration and hydrolysis time at a fixed oven temperature of 120 °C. In each case, reducing-sugar concentration increased toward the upper levels of the factors examined.

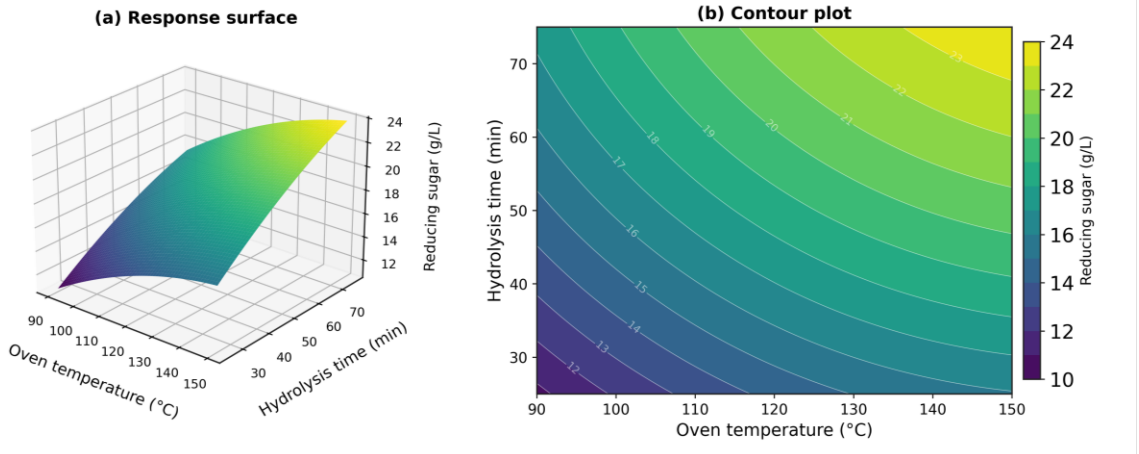

Figure 5: Response surface (a) and contour (b) plots for the combined effect of oven temperature and hydrolysis time on reducing-sugar concentration (acetic–citric acid = 2.00%).

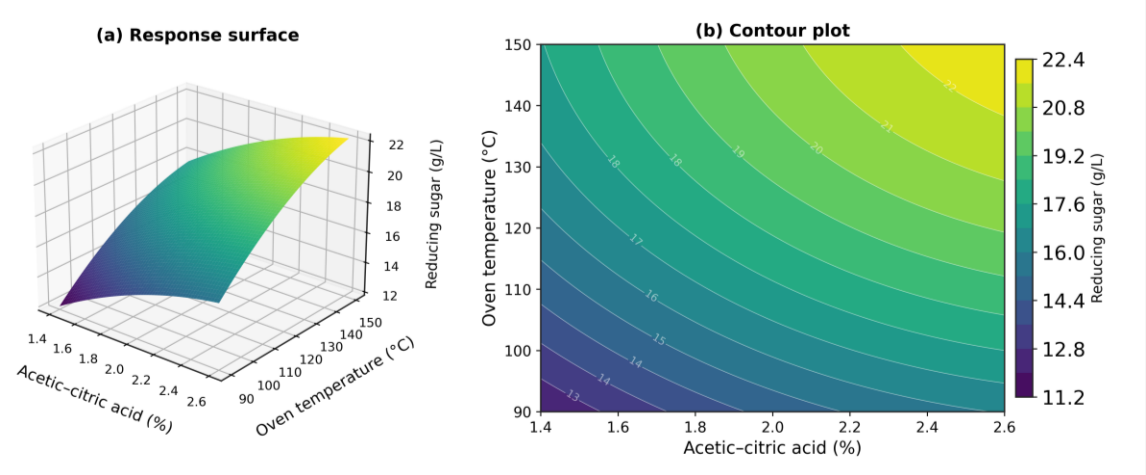

Figure 6: Response surface (a) and contour (b) plots for the combined effect of acetic–citric acid concentration and oven temperature on reducing-sugar concentration (hydrolysis time = 50 min).

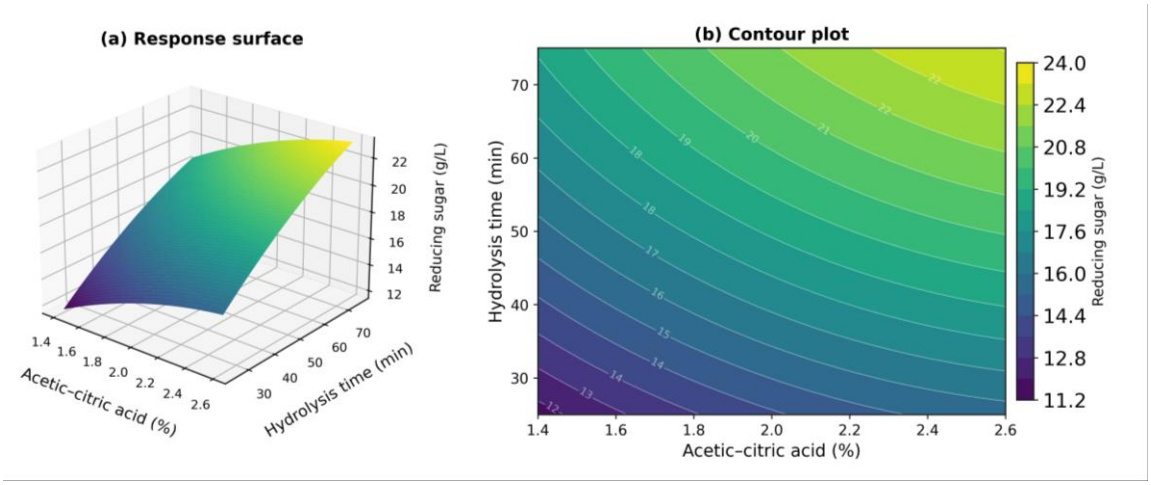

Figure 7: Response surface (a) and contour (b) plots for the combined effect of acetic–citric acid concentration and hydrolysis time on reducing-sugar concentration (oven temperature = 120 °C)

.

Optimization and validation

Numerical optimization was performed within the studied experimental region. The fitted quadratic surface increased toward the upper region of the design space, indicating that the mathematical stationary point of the model lay outside the experimental range. The selected high-yield validation condition was 2.72% acetic–citric acid, 151 °C and 78 min. Substitution of these values into the coded regression equation gave a predicted reducing-sugar concentration of 26.34 g/L. Triplicate validation under these conditions gave 24.63 ± 0.41 g/L, corresponding to an absolute difference of 1.71 g/L and a prediction error of 6.50%. The validated response was close to the highest experimental value in the design, confirming that the selected condition lay within the high-yield region of the fitted surface.

Table 4: Validation of the predicted high-yield hydrolysis condition (n = 3).

Parameter	Value
Acetic–citric acid concentration (%)	2.72
Oven temperature (°C)	151
Hydrolysis time (min)	78
Model-predicted reducing sugar (g/L)	26.34
Experimental reducing sugar (g/L)	24.63 ± 0.41
Absolute difference (g/L)	1.71
Prediction error (%)	6.50

Ethanol production from the optimized hydrolysate

The hydrolysate obtained under the optimized conditions was fermented with *Saccharomyces cerevisiae*. Ethanol concentration increased progressively during fermentation, from 2.84 g/L at 24 h through 5.37 g/L at 48 h and 7.46 g/L at 72 h to a maximum of 8.92 g/L at 96 h, followed by a slight decline to 8.61 g/L at 120 h (Table 5; Figure 8).

Table 5: Ethanol concentration during fermentation of the optimized cassava-peel hydrolysate.

Fermentation time (h)	Ethanol concentration (g/L)
24	2.84
48	5.37
72	7.46
96	8.92
120	8.61

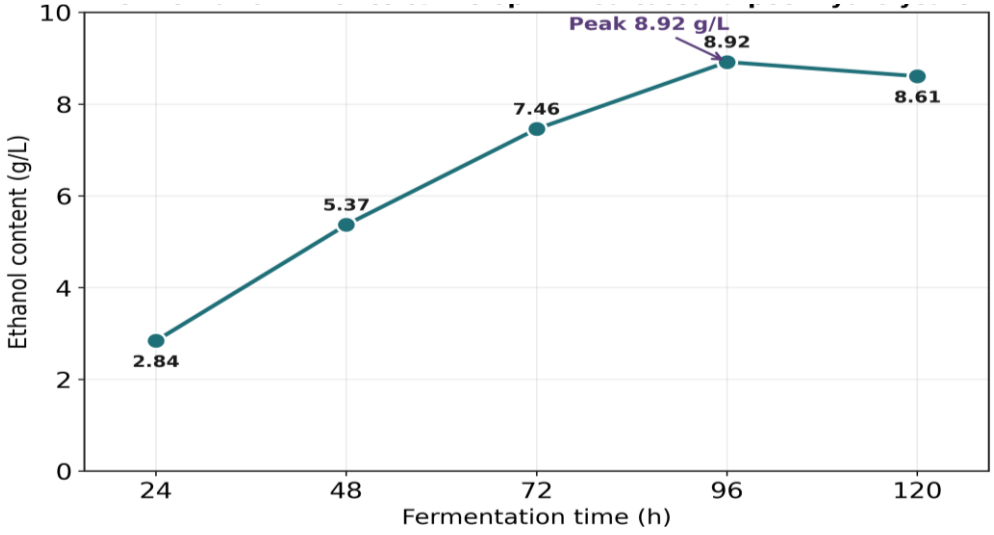

Figure 8: Ethanol concentration during fermentation of the optimized cassava peel hydrolysate with *Saccharomyces cerevisiae* over 120 h.

Summary of key findings

Under the modified central composite design, reducing-sugar concentration from oven-assisted acetic–citric acid hydrolysis of cassava peels ranged from 9.38 to 24.76 g/L, and a highly significant quadratic model ($R^2 = 0.9771$) described the data, with hydrolysis time and oven temperature exerting the strongest effects. The predicted high-yield condition (2.72% acid, 151 °C, 78 min; 26.34 g/L) was confirmed by triplicate validation (24.63 ± 0.41 g/L; 6.50% error), and fermentation of the optimized hydrolysate with *Saccharomyces cerevisiae* gave a maximum ethanol concentration of 8.92 g/L at 96 h (Table 6).

Table 6: Summary of the optimized hydrolysis and fermentation outputs.

Process stage	Optimized condition	Main output
Hydrolysis	2.72% acetic–citric acid, 151 °C, 78 min	Predicted 26.34 g/L; validated 24.63 ± 0.41 g/L RS
Fermentation	*S. cerevisiae*, 96 h	8.92 g/L ethanol

Discussion

The results show that a mixed acetic–citric acid system, applied under controlled oven heating, can release substantial fermentable sugar from cassava peel while keeping the chemistry comparatively mild. Reducing-sugar concentration rose monotonically with all three factors across the design space (9.38–24.76 g/L), and the second-order model accounted for almost all of the observed variation ($R^2 = 0.9771$; adjusted $R^2 = 0.9566$). The lack-of-fit was statistically significant ($p = 0.0001$); however, this outcome is driven by the exceptionally small pure error of the six center-point replicates (18.37–18.71 g/L; pure-error sum of squares = 0.102), which makes the lack-of-fit test acutely sensitive to even minor departures from the quadratic form. In practical terms, the model remained an accurate navigator of the design region, with a low coefficient of variation (5.18%), an adequate precision of 27.75, a predicted R^2 of 0.8353, and a validation error of only 6.50%. The significant lack-of-fit is nonetheless a genuine signal that the quadratic surface does not capture every feature of the response, and it is best resolved by augmenting the design (as noted in the final paragraph of the Discussion) rather than by over-interpreting the fitted coefficients. Comparable response surface and statistical-design approaches have been used to optimize dilute-acid and thermochemical processing of cassava and other agricultural residues, supporting the suitability of this framework for navigating cassava-peel hydrolysis (El-Imam, 2022; Igwebuike et al., 2024; Suriyachai et al., 2024).

The relative ranking of the three factors is mechanistically coherent. Hydrolysis time exerted the largest single effect, followed by oven temperature and then acid concentration, a pattern visible both in the partial sums of squares (Table 2) and in the divergence of the perturbation curves (Figure 4). In a starch–lignocellulosic residue such as cassava peel, sugar release is governed by the progressive hydration, swelling and cleavage of glycosidic bonds, processes that are kinetically limited and therefore strongly time- and temperature-dependent. Acetic and citric acids act primarily as proton donors that catalyze hydrolysis, but at the concentrations used here they contribute less to the overall response than the thermal driving force of the oven. None of the two-factor interactions reached significance, indicating that, within the window studied, the three factors acted largely independently rather than synergistically, so their effects are approximately additive. The significant negative quadratic terms for acid and temperature (A^2, B^2) point to diminishing returns at the upper levels of these factors, consistent with the depletion of readily hydrolysable substrate and the onset of

competing sugar-degradation reactions as severity increases; the non-significant time quadratic (C^2) implies that sugar release had not yet saturated over the 15–85 min window and remained close to linear in time.

Set against the cassava-peel literature, the present yields are best read alongside the differing process intent of each route rather than as a simple ranking. Igwebuike et al. (2024) obtained an optimized carbohydrate yield of about 0.76 g per gram of cassava peel by dilute-acid hydrolysis, and Papathoti et al. (2021) reported reducing-sugar yields near 670 mg/g with roughly 81% saccharification efficiency after alkali-assisted hydrothermal pretreatment followed by enzymatic hydrolysis. Such studies, together with the thermochemical optimization of cassava waste reported by Suriyachai et al. (2024) and comparative acid-versus-enzymatic screening (Chibuike et al., 2026), achieve high sugar release but rely on either added enzymes, alkaline reagents or more intensive thermochemical steps. The present route deliberately trades a portion of that maximum sugar release for operational simplicity and low toxicity, using only inexpensive food-grade acids and a standard laboratory oven. The reducing-sugar concentrations obtained here are therefore competitive within the mild end of this spectrum while requiring neither enzyme cocktails nor specialized reactors.

The principal advantage of the mild organic-acid strategy lies in what it avoids downstream. Severe dilute-mineral-acid and high-severity thermal pretreatments are well known to generate furfural, hydroxymethylfurfural and phenolic compounds that depress yeast viability and ethanol productivity, with furfural in particular impairing central metabolism and redox balance in *Saccharomyces cerevisiae* (Jilani & Olson, 2023; Yao et al., 2024). The persistence of these inhibitors has driven a substantial body of recent work dedicated to managing them: physical and nano-based detoxification of acid hydrolysates (Hong et al., 2021; Adebule et al., 2024), and dedicated removal of glucose-derived HMF during bioethanol production (Chizoma & Ize, 2025). In parallel, considerable effort has gone into engineering or selecting microorganisms that tolerate inhibitor-rich hydrolysates, including adaptive laboratory evolution of furfural-tolerant yeast (Yao et al., 2024), inhibitor-tolerant and xylose-fermenting engineered *S. cerevisiae* strains (Mokomele et al., 2023; Wu et al., 2023; Demeke et al., 2024), multistress-tolerant non-conventional yeasts for undetoxified hydrolysates (Klanrit et al., 2025; Yang et al., 2025), and co-cultivation with inhibitor-degrading partners that combine detoxification with fermentation (Acosta et al., 2021; Jawad et al., 2023; Liu et al., 2024). The redox stress imposed by such hydrolysates is significant enough to warrant dedicated biosensors for monitoring it during propagation and fermentation (Foncillas et al., 2023), and integrated first- and second-generation schemes have been devised partly to dilute inhibitor loads (De Oliveira Pereira et al., 2024).

Against that backdrop, the fermentation outcome observed here is informative. A maximum ethanol concentration of 8.92 g/L was reached within 96 h using ordinary commercial baker's yeast on the undetoxified hydrolysate, with *Saccharomyces cerevisiae* sustaining an uninterrupted rise in ethanol over the first four days rather than the prolonged lag phase characteristic of detoxification-limited fermentations. This behavior is consistent with a hydrolysate of low inhibitor burden and suggests that the mild acetic–citric window sidesteps much of the inhibitor problem that the strategies above were developed to solve. In effect, the process shifts the burden away from costly downstream detoxification or strain engineering and onto a simpler, gentler pretreatment, which is an attractive trade for low-resource settings. The ethanol yields reported for cassava peel under more intensive routes remain higher in absolute terms, for example around 0.29 g/g for dilute-acid hydrolysate co-fermented with *S. cerevisiae* and *Scheffersomyces stipitis* (Igwebuike et al., 2024) and up to 0.44 g/g for hydrothermally pretreated hydrolysate under simultaneous saccharification and fermentation (Papathoti et

al., 2021), but those gains come with the added reagents, enzymes or engineered organisms that the present route forgoes.

The fermentation profile itself follows the expected pattern for a batch yeast process. Ethanol accumulated rapidly between 24 and 96 h as the available sugars were consumed, after which the slight decline to 8.61 g/L at 120 h is attributable to the exhaustion of fermentable substrate combined with minor oxidative or assimilatory losses once the carbon source becomes limiting. The 96 h peak therefore defines the practical harvest point for this hydrolysate, and extending fermentation beyond it offers no benefit.

From an optimization standpoint, the model surface increased toward the upper corner of the experimental region, so the numerically identified condition (2.72% acid, 151 °C, 78 min) represents a high-yield operating point near the boundary rather than an interior stationary maximum. The validation experiment returned 24.63 ± 0.41 g/L against a model prediction of 26.34 g/L, a prediction error of 6.50%. While larger than would be expected for an interior optimum, this level of agreement is acceptable for a boundary condition and confirms that the model reliably locates the high-yield region. The modest over-prediction is consistent with the diminishing-returns behavior captured by the negative quadratic terms, which the extrapolation toward the design edge does not fully accommodate. For practical deployment, operating slightly inside this boundary would trade a small amount of sugar yield for greater robustness and lower thermal input.

Several limitations temper these conclusions and frame the next steps. First, the boundary location of the optimum, together with the statistically significant lack-of-fit, indicates that the current design does not fully bracket the response; a follow-up design that shifts the experimental window upward in temperature and time, adds replication away from the center, and thereby resolves the residual curvature would place the optimum on a firmer footing. Second, the study quantified reducing sugars and ethanol but did not directly measure inhibitor concentrations; explicit determination of furfural, hydroxymethylfurfural and phenolics would substantiate the inferred low-inhibitor advantage of the organic-acid route and allow direct comparison with the detoxification and tolerance studies cited above (Jilani & Olson, 2023; Adebule et al., 2024; Klanrit et al., 2025). Third, fermentation was conducted only on the optimized hydrolysate with a single commercial yeast, so the generality of the ethanol performance across hydrolysates of differing severity, and against inhibitor-tolerant or co-culture systems, remains to be established (Acosta et al., 2021; Jawad et al., 2023; Wu et al., 2023). Addressing these points, alongside an economic and energy analysis of the oven-heating step and scale-up beyond flask volumes, would strengthen the case for oven-assisted acetic–citric hydrolysis as a low-barrier valorization route for cassava peel waste.

Conclusion

Oven-assisted hydrolysis of cassava peel with a mixed acetic–citric acid system, optimized by response surface methodology, proved an effective and laboratory-accessible route to fermentable sugars and bioethanol. The optimized condition (2.72% acetic–citric acid, 151 °C, 78 min) gave a validated reducing-sugar concentration of 24.63 ± 0.41 g/L, and subsequent fermentation with *Saccharomyces cerevisiae* produced a maximum ethanol concentration of 8.92 g/L at 96 h. The mild, low-toxicity nature of the organic-acid system, combined with its reliance on simple oven heating and food-grade reagents, makes it an attractive option for valorizing cassava peel waste. Because the optimum lay near the edge of the design and the model showed a significant lack-of-fit, future work should extend the experimental window to bracket the optimum, quantify inhibitor formation, test a wider range of fermentation conditions and yeasts, and evaluate the energy economics and scalability of the process.

Acknowledgement

The authors thank the Biotechnology and Product Development Department, National Root Crops Research Institute (NRCRI), Umudike, and the PG laboratory of the Department of Microbiology, Michael Okpara University of Agriculture, Umudike, for laboratory support and access to facilities.

No corporate or individual funding was received for this research.

Conflict of Interest

The authors declare that there is no conflict of interest regarding the publication of this paper.

Author Contribution

The authors confirm contribution to the paper as follows: study design: Onwuakor, C. E.; data collection: Nwokafor, C. V.; analysis and interpretation of results: Onwuakor, C. E., Nwokafor, C. V.; draft manuscript preparation: Onwuakor, C. E., Nwokafor, C. V. Both authors reviewed the results and approved the final version of the manuscript.

References

Acosta, A. M., Cosovanu, D., López, P. C., Thomsen, S. T., Gernaey, K. V., & Canela-Garayoa, R. (2021). Co-cultivation of a novel *Fusarium striatum* strain and a xylose consuming *Saccharomyces cerevisiae* yields an efficient process for simultaneous detoxification and fermentation of lignocellulosic hydrolysates. Chemical Engineering Journal, 426, 131575. https://doi.org/10.1016/j.cej.2021.131575

Adebule, A. P., Sanusi, I. A., & Kana, E. G. (2024). Nano-based surface adsorption detoxification of process inhibitors for improved bioethanol productivity. Bioresource Technology Reports, 25, 101783. https://doi.org/10.1016/j.biteb.2024.101783

Ariffin, K. K., Masngut, N., Seman, M. N. A., Saufi, S. M., Jamek, S., & Sueb, M. S. M. (2020). Dilute acid hydrolysis pretreatment for sugar and organic acid production from pineapple residues. IOP Conference Series Materials Science and Engineering, 991(1), 012057. https://doi.org/10.1088/1757-899x/991/1/012057

Awogbemi, O., & Von Kallon, D. V. (2022). Valorization of agricultural wastes for biofuel applications. Heliyon, 8(10), e11117. https://doi.org/10.1016/j.heliyon.2022.e11117

Broda, M., Yelle, D. J., & Serwańska, K. (2022). Bioethanol Production from Lignocellulosic Biomass—Challenges and Solutions. Molecules, 27(24), 8717. https://doi.org/10.3390/molecules27248717

Cheng, J., Huang, C., Huang, C., Zhan, Y., Liu, X., Wang, J., Huang, C., Huang, C., Fang, G., Ragauskas, A. J., Xie, Z., & Meng, X. (2023). A novel mineral-acid free biphasic deep eutectic solvent/γ-valerolactone system for furfural production and boosting the enzymatic hydrolysis of lignocellulosic biomass. Bioresource Technology, 387, 129653. https://doi.org/10.1016/j.biortech.2023.129653

Chibuike, G., Onyegeme-Okerenta, B., Wegwu, M. O., Nwikiri, B., & Ibegbulem, C. (2026). A comparative study of acid and enzymatic pre-treatment of selected agricultural waste materials for bioethanol production. African Journal of Health Safety and Environment, 7(1), 104–113. https://doi.org/10.52417/ajhse.v7i1.687

Chizoma, A., & Ize, Y. M. (2025). Effects of Different Detoxification Methods on Glucose and Hydroxymethyfurfural (HMF) during Bioethanol Production. International Research Journal of Modernization in Engineering Technology and Science. https://doi.org/10.56726/irjmets81803

Chukwudi, K., Otaraku, I., & Muwarure, P. (2025). Compositional analysis and hydrothermal pretreatment optimization of GaRRi processing waste for enhanced sugar recovery. International Journal on Science and Technology, 16(4). https://doi.org/10.71097/ijsat.v16.i4.9429

De Oliveira Pereira, I., Santos, Â. a. D., Guimarães, N. C., Lima, C. S., Zanella, E., Matsushika, A., Rabelo, S. C., Stambuk, B. U., & Ienczak, J. L. (2024). First- and second-generation integrated process for bioethanol production: Fermentation of molasses diluted with hemicellulose hydrolysate by recombinant *Saccharomyces cerevisiae*. Biotechnology and Bioengineering, 121(4), 1313–1323. https://doi.org/10.1002/bit.28648

Demeke, M. M., Echemendia, D., Belo, E., Foulquié-Moreno, M. R., & Thevelein, J. M. (2024). Enhancing xylose-fermentation capacity of engineered *Saccharomyces cerevisiae* by multistep evolutionary engineering in inhibitor-rich lignocellulose hydrolysate. FEMS Yeast Research, 24. https://doi.org/10.1093/femsyr/foae013

Dharmalingam, B., Tantayotai, P., Panakkal, E. J., Cheenkachorn, K., Kirdponpattara, S., Gundupalli, M. P., Cheng, Y., & Sriariyanun, M. (2022). Organic Acid Pretreatments and Optimization Techniques for Mixed Vegetable Waste Biomass Conversion into Biofuel Production. BioEnergy Research, 16(3), 1667–1682. https://doi.org/10.1007/s12155-022-10517-y

Du Pasquier, J., Paës, G., & Perré, P. (2024). Chemical degradation, yields, and interactions of lignocellulosic compounds of poplar wood during dilute acid pretreatment assessed from a comprehensive data set. Industrial Crops and Products, 215, 118643. https://doi.org/10.1016/j.indcrop.2024.118643

El-Imam, A. A. (2022). Optimisation of dilute acid hydrolysis for bioethanol production from selected agricultural wastes. SLU Journal of Science and Technology, 5(1 & 2), 13–20. https://doi.org/10.56471/slujst.v5i.244

Escobar, E. L. N., Da Silva, T. A., Pirich, C. L., Corazza, M. L., & Ramos, L. P. (2020). Supercritical fluids: a promising technique for biomass pretreatment and fractionation. Frontiers in Bioengineering and Biotechnology, 8, 252. https://doi.org/10.3389/fbioe.2020.00252

Foncillas, R. P., Sebastiá, M. S., Wallberg, O., Carlquist, M., & Gorwa-Grauslund, M. F. (2023). Assessment of the TRX2p-yEGFP Biosensor to Monitor the Redox Response of an Industrial Xylose-Fermenting *Saccharomyces cerevisiae* Strain during Propagation and Fermentation. Journal of Fungi, 9(6), 630. https://doi.org/10.3390/jof9060630

Gönen, Ç., Deveci, E. Ü., & Önal, N. A. (2021). Evaluation of biomass pretreatment to optimize process factors for different organic acids via Box–Behnken RSM method. Journal of Material Cycles and Waste Management, 23(5), 2016–2027. https://doi.org/10.1007/s10163-021-01276-7

Holmatov, B., Schyns, J., Krol, Gerbens-Leenes, P., & Hoekstra, A. (2021). Can crop residues provide fuel for future transport? Limited global residue bioethanol potentials and large associated land, water and carbon footprints. Renewable and Sustainable Energy Reviews, 149, 111417. https://doi.org/10.1016/j.rser.2021.111417

Honarmandrad, Z., Kucharska, K., Kaykhaii, M., & Gębicki, J. (2024). Removal of phenolic inhibitor compounds from hydrolysates and post-fermentation broths by using a hydrophobic magnetic deep eutectic solvent. Journal of Environmental Chemical Engineering, 12(3), 112621. https://doi.org/10.1016/j.jece.2024.112621

Hong, J., Gam, D., Kim, J., Kim, J., Jeon, S., Kim, H., Kim, J., & Kim, J. (2021). Process Development for the Detoxification of Fermentation Inhibitors from Acid Pretreated Microalgae Hydrolysate. Molecules, 26(9), 2435. https://doi.org/10.3390/molecules26092435

Igwebuike, C. M., Awad, S., & Andrès, Y. (2024). Bioethanol production from dilute acid hydrolysis of cassava peels, sugar beet pulp, and green macroalgae (*Ulva lactuca*). Biofuels, 15(9), 1145–1157. https://doi.org/10.1080/17597269.2024.2336328

Jawad, M., Wang, H., Wu, Y., Rehman, O., Song, Y., Xu, R., Zhang, Q., Gao, H., & Xue, C. (2023). Lignocellulosic ethanol and butanol production by *Saccharomyces cerevisiae* and *Clostridium beijerinckii* co-culture using non-detoxified corn stover hydrolysate. Journal of Biotechnology, 379, 1–5. https://doi.org/10.1016/j.jbiotec.2023.11.002

Jayakumar, M., Gindaba, G. T., Gebeyehu, K. B., Periyasamy, S., Jabesa, A., Baskar, G., John, B. I., & Pugazhendhi, A. (2023). Bioethanol production from agricultural residues as lignocellulosic biomass feedstock's waste valorization approach: A comprehensive review. The Science of the Total Environment, 879, 163158. https://doi.org/10.1016/j.scitotenv.2023.163158

Jilani, S. B., & Olson, D. G. (2023). Mechanism of furfural toxicity and metabolic strategies to engineer tolerance in microbial strains. Microbial Cell Factories, 22(1), 221. https://doi.org/10.1186/s12934-023-02223-x

Klanrit, P., Thanonkeo, S., Pilap, W., Apiraksakorn, J., Fiala, K., Leesing, R., Yamada, M., & Thanonkeo, P. (2025). Optimization of Fermentation Parameters for Enhanced Bioethanol Production by Multistress-Tolerant *Saccharomycodes ludwigii* APRE2 Using Undetoxified Sugarcane Bagasse Hydrolysate. Energies, 18(13), 3428. https://doi.org/10.3390/en18133428

Koul, B., Yakoob, M., & Shah, M. P. (2021). Agricultural waste management strategies for environmental sustainability. Environmental Research, 206, 112285. https://doi.org/10.1016/j.envres.2021.112285

Liu, C., Choi, B., Efimova, E., Nygård, Y., & Santala, S. (2024). Enhanced upgrading of lignocellulosic substrates by coculture of *Saccharomyces cerevisiae* and *Acinetobacter baylyi* ADP1. Biotechnology for Biofuels and Bioproducts, 17(1), 61. https://doi.org/10.1186/s13068-024-02510-8

Mardina, P., Irawan, C., Putra, M. D., Priscilla, S. B., Misnawati, M., & Nata, I. F. (2021). Bioethanol Production from Cassava Peel Treated with Sulfonated Carbon Catalyzed Hydrolysis. Jurnal Kimia Sains Dan Aplikasi, 24(1), 1–8. https://doi.org/10.14710/jksa.24.1.1-8

Mokomele, T., Brandt, B. A., & Görgens, J. F. (2023). Effective Fermentation of Sugarcane Bagasse Whole Slurries Using Robust Xylose-Capable *Saccharomyces cerevisiae*. BioEnergy Research, 16(4), 2297–2313. https://doi.org/10.1007/s12155-023-10577-8

Osemwengie, S., Osagie, E., & Onwukwe, B. (2021). Optimization of bioethanol production from cassava peels. Journal of Applied Science and Environmental Management, 24(12), 2077–2083. https://doi.org/10.4314/jasem.v24i12.11

Papathoti, N. K., Laemchiab, K., Megavath, V. S., Keshav, P. K., Numparditsub, P., Thanh, T. L., & Buensanteai, N. (2021). Augmented ethanol production from alkali-assisted hydrothermal pretreated cassava peel waste. Energy Sources Part a Recovery Utilization and Environmental Effects, 47(1), 8243–8253. https://doi.org/10.1080/15567036.2021.1928338

Permatasari, N. U., Dali, S., & Wahyuni, E. S. (2023). Potential Cassava Peel Waste (*Manihot esculenta* Crantz) in The Production of Bioethanol by Enzymatic Hydrolysis and Fermentation Using *Zymomonas mobilis* Bacteria. The Journal of Pure and Applied Chemistry Research, 12(2), 87–103. https://doi.org/10.21776/ub.jpacr.2023.012.02.3304

Suriyachai, N., Imman, S., Kreetachat, T., Laosiripojana, N., Khongchamnan, P., Champreda, V., Suwannahong, K., Sakulthaew, C., Chokejaroenrat, C., & Kreetachat, N. (2024). Enhanced bioethanol production from cassava waste: optimization of thermochemical pretreatment for maximum sugar recovery and characterisation of potential fractions. International Journal of Sustainable Energy, 43(1).

https://doi.org/10.1080/14786451.2024.2411833

Świątek, K., Gaag, S., Klier, A., Kruse, A., Sauer, J., & Steinbach, D. (2020). Acid hydrolysis of lignocellulosic biomass: sugars and furfurals formation. Catalysts, 10(4), 437. https://doi.org/10.3390/catal10040437

Thuppahige, V. T. W., Moghaddam, L., Welsh, Z. G., Wang, T., & Karim, A. (2023). Investigation of critical properties of Cassava (*Manihot esculenta*) peel and bagasse as starch-rich fibrous agro-industrial wastes for biodegradable food packaging. Food Chemistry, 422, 136200. https://doi.org/10.1016/j.foodchem.2023.136200

Wood, I. P., Elliston, A., Ryden, P., Bancroft, I., Roberts, I. N., & Waldron, K. W. (2012). Rapid quantification of reducing sugars in biomass hydrolysates: Improving the speed and precision of the dinitrosalicylic acid assay. Biomass and Bioenergy, 44, 117–121. https://doi.org/10.1016/j.biombioe.2012.05.003

Woźniak, A., Kuligowski, K., Świerczek, L., & Cenian, A. (2025). Review of lignocellulosic biomass pretreatment using physical, thermal and chemical methods for higher yields in bioethanol production. Sustainability, 17(1), 287. https://doi.org/10.3390/su17010287

Wu, Y., Su, C., Zhang, G., Liao, Z., Wen, J., Wang, Y., Jiang, Y., Zhang, C., & Cai, D. (2023). High-Titer Bioethanol Production from Steam-Exploded Corn Stover Using an Engineering *Saccharomyces cerevisiae* Strain with High Inhibitor Tolerance. Fermentation, 9(10), 906. https://doi.org/10.3390/fermentation9100906

Yang, Y., Li, X., Wang, Z., Deng, Y., Wang, Z., Fang, X., Zhang, M., Sun, W., Zhao, X., Liu, Z., & Zhang, F. (2025). Whole Genome Sequencing of *Kodamaea ohmeri* SSK and Its Characterization for Degradation of Inhibitors from Lignocellulosic Biomass. Biology, 14(5), 458. https://doi.org/10.3390/biology14050458

Yao, L., Jia, Y., Zhang, Q., Zheng, X., Yang, H., Dai, J., & Chen, X. (2024). Adaptive laboratory evolution to obtain furfural tolerant *Saccharomyces cerevisiae* for bioethanol production and the underlying mechanism. Frontiers in Microbiology, 14, 1333777. https://doi.org/10.3389/fmicb.2023.1333777